Mutation of a Major Keratin Phosphorylation Site Predisposes to Hepatotoxic Injury in Transgenic Mice

Nam-On Ku,*‖ Sara A. Michie,‡‖ Roy M. Soetikno,*‖ Evelyn Z. Resurreccion,‡‖ Rosemary L. Broome,§‖ and M. Bishr Omary*‖

*Department of Medicine, ‡Department of Pathology, and §Department of Veterinary Medicine, Veterans Administration Palo Alto Health Care System, Palo Alto, CA 94304; and the ‖Digestive Disease Center, Stanford University School of Medicine, Palo Alto, California 94305

Abstract. Simple epithelia express keratins 8 (K8) and 18 (K18) as their major intermediate filament (IF) proteins. One important physiologic function of K8/18 is to protect hepatocytes from drug-induced liver injury. Although the mechanism of this protection is unknown, marked K8/18 hyperphosphorylation occurs in association with a variety of cell stresses and during mitosis. This increase in keratin phosphorylation involves multiple sites including human K18 serine-(ser)52, which is a major K18 phosphorylation site. We studied the significance of keratin hyperphosphorylation and focused on K18 ser52 by generating transgenic mice that overexpress a human genomic K18 ser52→ala mutant (S52A) and compared them with mice that overexpress, at similar levels, wild-type (WT) human K18. Abrogation of K18 ser52 phosphorylation did not affect filament organization after partial hepatectomy nor the ability of mouse livers to regenerate. However, exposure of S52A-expressing mice to the hepatotoxins, griseofulvin or microcystin, which are associated with K18 ser52 and other keratin phosphorylation changes, resulted in more dramatic hepatotoxicity as compared with WT K18-expressing mice. Our results demonstrate that K18 ser52 phosphorylation plays a physiologic role in protecting hepatocytes from stress-induced liver injury. Since hepatotoxins are associated with increased keratin phosphorylation at multiple sites, it is likely that unique sites aside from K18 ser52, and phosphorylation sites on other IF proteins, also participate in protection from cell stress.

Key words: keratins • phosphorylation • intermediate filaments • transgenic mice • liver

Intermediate filament (IF)[1] proteins are one of the three major cytoskeletal protein groups, that also include microfilaments and microtubules (reviewed in reference 14, 34, 49). A comparison of the three major cytoskeletal protein groups shows several distinguishing unique features of IF proteins: they have nuclear (i.e., the lamins) and many cytoplasmic members, their cytoplasmic members appear to be expressed only in higher eucaryotes in a tissue preferential manner, and mutations of IF proteins cause a variety of human diseases (15). Among the diverse IF protein family, the keratin subgroup is the largest and is specifically expressed in epithelial cells (44). Aside from the "hard" keratins that are found in epidermal appendages (e.g., hair and nails), the "soft" keratins (K) consist of >20 members that are divided into relatively basic type II (K1-K8) and acidic type I (K9-K20) keratins (44). All epithelial cells express at least one type I and one type II keratin that associate, noncovalently, to form extended filamentous arrays. In general, epithelial cells express a dominant unique keratin pair depending on the epithelial cell type. For example, glandular epithelia express K8 and K18 (with variable levels of K19 and K20), whereas keratinocytes preferentially express K5/14 basally and K1/10 suprabasally. Although keratin function(s) remain poorly understood, one clear function is to provide mechanical integrity to cells including those in epidermis (15), cornea (19) and liver (46). This was clearly demonstrated by the phenotypes of several human diseases that are caused by keratin mutations and by several transgenic animal models that express mutant keratins (15, 43, 46).

All IF proteins have a prototype structure consisting of a central coiled-coil α–helix (310–350 amino acids) that is surrounded by globular NH_2-terminal head and COOH-

Address correspondence to Bishr Omary, Palo Alto VA Medical Center, 3801 Miranda Avenue, 154J, Palo Alto, CA 94304. Fax: (415) 852-3259.

Address reprint requests to Nam-On Ku, Palo Alto VA Medical Center, 3801 Miranda Avenue, 154J, Palo Alto, CA 94304. Fax: (415) 852-3259.

1. *Abbreviations used in this paper:* Emp, Empigen BB; GF, griseofulvin; IF, intermediate filament(s); K, keratin; MLR, microcystin LR; pS, phospho-serine; PVDF, polyvinylidene difluoride; S52A, transgenic mice that overexpress ser52→ala K18; TG2, transgenic mice that overexpress wild-type human K18; WT, wild-type.

terminal tail domains of variable length (14, 34, 49). The globular end domains provide most of the structural heterogeneity among IF proteins and contain all currently known phosphorylation and glycosylation sites, in contrast with the nonmodified rod domain (reviewed in 18, 26, 47). The exclusive presence of keratin phosphorylation within the structurally heterogeneous head and tail domains suggests that this modification may play a regulatory role in the presumed tissue-specific function of these proteins. In the case of K18, ser52 is its major phosphorylation site during interphase. K18 ser52 phosphorylation is highly dynamic, increases two to three times during mitosis, and appears to be important for filament reorganization (23, 37). A potential role for K18 ser52 in filament organization was implicated based on transfection of a K18 ser52→ala mutant, which results in a keratin filamentous array that is twofold less able to reorganize its filaments, after treatment with colcemid or okadaic acid, as compared with WT K18-transfected cells (23). Several other K8 and K18 phosphorylation sites have been identified including K18 ser33 that regulates binding to 14-3-3 proteins (30), K8 ser23 that is highly conserved among all type II keratins (24), K8 ser431 that is phosphorylated by MAP kinase upon EGF stimulation (24), and K8 ser73 that becomes phosphorylated during mitosis, cell stress, and apoptosis (40).

Two observations led us to investigate keratin phosphorylation in transgenic mice in situ. First, disruption of K8/18 filaments in transgenic mice after expression of a dominant negative K18 arg89→cys results in hepatocyte keratin IF collapse in association with chronic hepatitis (25) and increased susceptibility to drug-induced liver injury (27). This, coupled with the abnormal liver phenotype of K8-null mice (4, 5, 41) and mice that express K14 ectopically in the liver (3) indicated that K8/18 play an important role in helping hepatocytes cope with cell stress. Such a functional role for keratin was not discernible before the use of transgenic animal models as was done first for K14 (54) and subsequently several other IF proteins (15), and the initial identification of keratin mutations in the human blistering skin disease epidermolysis bullosa simplex (6, 13, 33). Second, a variety of stress conditions in cultured cells and intact animals are associated with significant K8/18 hyperphosphorylation, including rotavirus infection or heat stress in cultured cells (38), apoptosis (8, 28), and drug-induced liver injury using the anti-fungal agent griseofulvin (27) or the phosphatase inhibitor microcystin LR (MLR; 45, 51, 52). Given that ser52 is a major K18 phosphorylation site, we sought to determine its physiologic function by generating transgenic mice that overexpress a K18 ser52→ala mutant and comparing the phenotype and keratin phosphorylation in these mice with the well described transgenic mice that overexpress WT human K18 (termed TG2; references 1, 25, 27). This represents the first report that we are aware of that utilizes transgenic animals to study the significance of a single phosphorylation site of a protein.

Materials and Methods

Cell Culture, Antibodies, and Reagents

NIH-3T3 (mouse fibroblast) and HT29 (human colon) cells (American Type Culture Collection, Manassas, VA) were cultured as recommended by the supplier. Antibodies (Ab) used were: L2A1 mouse mAb that recognizes human K18 without cross-reacting with mouse keratins (11, 25); Troma I rat mAb that recognizes mouse K8 (Developmental Studies Hybridoma Bank, University of Iowa, Iowa City, IA); rabbit Ab 8592 that was raised against human K8/18 (25); rabbit Ab 3055 that recognizes phospho-ser52 (pS52) of human K18 and does not cross-react with the corresponding phosphorylation site in mouse K18 that has a different antigenic context (37); rabbit Ab 8250 that recognizes human K18 pS33 and does cross-react with the equivalent mouse phosphorylation site (30); mAb LJ4 that recognizes K8 pS73 (40); anti-mouse K18 (provided by Robert Oshima); and anti-plectin and anti-desmoplakin Abs (provided by Harald Herrmann and Manijeh Pasdar, respectively). Other reagents used were: microcystin-LR (Alexis Corp., San Diego, CA), griseofulvin (GF; Sigma Chemical Company, St. Louis, MO), calf intestine alkaline phosphatase (Boehringer Mannheim, Indianapolis, IN), orthophosphate ($^{32}PO_4$; Dupont-New England Nuclear, Wilmington, DE), Empigen (Emp) BB detergent (Calbiochem-Novabiochem Corp., La Jolla, CA), collagenase type I (Worthington Biomedical Corp., Freehold, NJ), Transformer™ mutagenesis kit (CLONTECH Laboratories, Palo Alto, CA), and powdered Lab Diet (PMI Feeds Inc., St. Louis, MO).

Transgene Construct and Generation of Transgenic Lines

The human K18 cDNA ser52 codon (AGC) was mutated to a GCC (ala) codon in a pBluescript SK+ plasmid using the Transformer kit as recommended by the manufacturer. Confirmation of the mutation was done by sequencing both strands of the mutated region. The mutant cDNA was then digested with AlwN I to generate a 250-bp fragment that was then substituted for the corresponding wild-type segment of exon 1 in a 10-kb genomic K18 clone (provided by Dr. Robert Oshima, The Burnham Institute, La Jolla, CA), exactly as we had done in generating the arg89→cys K18 genomic mutant (25). The 10-kb K18 ser52→ala genomic DNA was injected into pronuclei of fertilized FVB/N mouse eggs. Progeny mice carrying the human K18 gene were then chosen, after PCR screening, followed by breeding to select for germline transmission using standard methods. Two mouse lines ($S52A^1$ and $S52A^2$) that express K18 ser52→ala were expanded and used for subsequent studies. The control mice that were used (TG2 mice) overexpressed the wild-type 10-kb genomic K18 (1, 25, 27). PCR screening of mouse tail genomic DNA for the presence of human K18 involved amplification of a 270-bp fragment that corresponds to the COOH-terminal region of K18. The primers used were: (+) 5′-CAGAAGGCCAGCTTGGAGAAC-3′ and (−) 5′-ATCTCCTGATCCCAGCACGTG-3′. All mice were housed in the same room with standard infection control precautions.

Transgenic Mice, Liver and Serum Testing, and Partial Hepatectomy

For all transgenic mouse hepatectomy and liver toxicity experiments, age (all >6 wk old, no more than 2 wk difference in age among the various groups) and sex-matched mice were weighed just before use. Liver and blood were collected after killing the mice using CO_2 inhalation, then bleeding via intracardiac puncture (0.5–1.0 ml). The liver was them immediately harvested. Serum was analyzed from TG2 and $S52A^1$ and $S52A^2$ control diet-fed mice (8 mice/line), GF-fed TG2 and $S52A^1$ mice (10 mice/line), MLR-treated mice (10 mice/line) for creatinine, glucose, total protein, alkaline phosphatase, albumin, triglycerides, cholesterol, total bilirubin, and alanine and aspartate aminotransferases. Partial hepatectomy was done by removing the lateral, left, and right median lobes, as described (55, 56) from TG2, $S52A^1$ and $S52A^2$ mice (16 mice/per transgenic line). Mice were then killed 24 h (4 mice/line), 48 h (6 mice/line), and 72 h (6 mice/line) afterwards and the livers were processed as below. For the hepatectomy experiments, sham-hepatectomized mice (i.e., mice that had anesthesia, an abdominal wall and peritoneal incision, exposure of the liver then closure of the incisions) from each transgenic line served as controls. Resected livers (from control diet-fed, sham-hepatectomized, post-hepatectomy, GF-fed, or MLR-administered) were cut into several pieces depending on the experiment and used for one or more of the following: (*a*) fixation with 10% formalin followed by paraffin embedding, sectioning, then hematoxylin and eosin staining (done by Histo-tec Laboratory, Hayward, CA), (*b*) snap freezing in O.C.T. compound, sectioning then fixing briefly in cold acetone for subsequent immunofluorescence staining, (*c*) snap freezing in liquid nitrogen for subsequent biochemical analysis,

and (*d*) cutting into small fragments then metabolic labeling with $^{32}PO_4$ in phosphate-free medium. Liver perfusion was performed as described (12) using 0.025% collagenase type I, and hepatocyte viability was determined using trypan blue exclusion.

Griseofulvin and Microcystin-LR Experiments

A pilot experiment was initially done using TG2, S52A[1], and S52A[2] mice that were fed powered diet ±1.25% GF (6 mice/group). Since both S52A[1] and S52A[2] mice gave similar results in terms of having a worse histologic score upon GF feeding as compared with TG2 mice, we only used the S52A[1] for subsequent experiments. Mice (10/line) were then fed control or GF-supplemented diet for 17 d followed by isolation, weighing then processing of the livers as described above. Alternatively, mice were fed control or GF-containing diet for 2, 5, or 8 d (2 mice/line) followed by the processing of the livers. For the MLR experiments, pilot experiments were carried out to determine the optimal dose that does not cause rapid lethality. A dose of 30 μg/Kg was chosen, and as found for the GF experiments, the S52A[1] and S52A[2] had a worse histology than the TG2 mice that led us to use the S52A[1] line for the subsequent quantitative experiments. Mice (10/line) from each group were given 30 μg/Kg of MLR intraperitoneally, followed by processing of the livers after 195 min. MLR was prepared in dimethylsulfoxide, as a 1 mg/ml stock solution, then diluted in PBS (10 mM sodium phosphate/0.15 M NaCl, pH 7.4).

Histology Grading and Statistical Analysis

All histology slides were examined by a pathologist (S.A. Michie) without knowledge of the treatment, diet, or transgenic line. Grading of the GF-related slides was done by counting the number of necrotic cells in a 20× field (10 fields per slide) and is presented as a necrosis score. Grading of the MLR-related slides was done by estimating the extent of vacuolization (*vacuolization score*) and area of hemorrhage/necrosis (*hemorrhage score*). The vacuole score was estimated by assigning a 0 to 3+ score depending on the percentage of vacuole volume as compared with overall hepatocyte cytoplasmic volume such that: 0 = <10%, 1+ = 10–29%, 2+ = 30–49%, and 3+ = ≥50%. The hemorrhage score was estimated by assigning a 0 to 3+ score depending on extent of the hemorrhage and necrosis: 0 = no necrosis, 1+ = small foci (mostly midzonal), 2+ = confluent areas, and 3+ = diffuse hemorrhage and necrosis with rare intact islands of hepatocytes. All scores and laboratory parameters are expressed as means ±SD. The Student's *t* test and nonparametric Wilcoxon method were used to calculate the statistical significance between the means. Statistical analysis was performed using JMP version 3.1 (SAS Institute Inc., Cary, NC).

Keratin Isolation, Immunoprecipitation, and Other Methods

Liver pieces (~3 × 4 × 4 mm) were used to isolate keratins exactly as described previously, either by immunoprecipitation (26) or high salt extraction (2, 25) except that NaF and sodium pyrophosphate were not added to the solubilization buffer. For immunoprecipitation, liver pieces were solubilized in 1% Emp or 1% NP-40 in PBS containing a protease/phosphatase inhibitor cocktail (25). Dephosphorylation of keratin immunoprecipitates was done with alkaline phosphatase (20 units/μl stock enzyme mix) using 20 units in 20 μl of buffer (supplied by the manufacturer with the enzyme) for 1 h (30°C) followed by washing 2× with 1% NP-40 in PBS. SDS-PAGE was done using 10% acrylamide gels (31). Radiolabeling of NIH-3T3 or HT29 cells, or liver tissue fragments (250 μCi/ml) was done in 5 ml or 2 ml, respectively, of phosphate free RPMI-1640 media containing 10% dialyzed FCS and 1–2% normal medium. Immunoblotting (53) was done by transferring immunoprecipitates or total cell lysates (solubilized in 2% SDS/5% glycerol-containing Laemmli sample buffer) to polyvinylidene difluoride (PVDF) membranes followed by blotting with 1:1,000 dilution of anti-keratin antibodies then visualization of the reactive bands using enhanced chemiluminescence. Tryptic phosphopeptide mapping of K18 that was purified by immunoprecipitation from $^{32}PO_4$-prelabeled detergent solubilized HT29 or transfected NIH-3T3 cells or mouse freshly isolated liver fragments was done exactly as described (7). IEF of the keratin precipitates (39) was done using a Mini-PROTEAN II apparatus (BioRad Laboratories, Cambridge, MA) and an ampholine pH mix of 3-10 and 5-7 as recommended by the manufacturer. Immunofluorescence staining was done as described (26).

Comparative quantitation of keratin protein levels and phosphorylation was done using densitometric scanning of Coomassie-stained gels, or by immunoblotting of serial dilutions of total liver tissue homogenates using anti-pankeratin or anti-phosphokeratin antibodies. Northern blot analysis was done using total liver RNA.

Results

Characterization of Transgenic Mice That Overexpress Human K18 ser52→ala

To address the physiologic function of keratin phosphorylation, we targeted a specific keratin phosphorylation site in the context of an intact transgenic mouse. Our hypothesis was that transgene expression of a keratin that is mutated at a particular phosphorylation site may clarify the potential role of keratin phosphorylation during mitosis and/or in providing protection from drug-induced liver injury. This hypothesis is based on the increase in K8/18 phosphorylation that is observed in association with a variety of cell stresses in mice and cultured cells (26, 47). To test this hypothesis, we generated a genomic K18 ser52→ala mutant and injected it into mouse embryos then selected two lines (S52A[1] and S52A[2]). The wild-type (WT) 10-kb genomic K18 construct that we used to generate the point mutation was identical to what we used previously to generate a genomic K18 arg89→cys, which afforded tissue specific overexpression of human K18 that paralleled that of the endogenous mouse K18 (25). For comparison, and to serve as a control for WT human K18 overexpression, we used the well-characterized TG2 mice that overexpress WT human K18 (1, 25). To isolate the overexpressed human keratin, we used mAb L2A1 that recognizes human K18 and does not cross-react with mouse keratins (25). As shown in Fig. 1 *A*, mAb L2A1 immunoprecipitated nearly equal levels of keratins from livers of TG2 mice and mice from the two S52A transgenic lines. As would be expected, immunoblotting of these precipitates with the previously described Ab 3055, which specifically recognizes an epitope that contains human phospho-ser52 (pS52; reference 37), showed binding only to K18 from TG2 mice but not to K18 from S52A mice (Fig. 1 *A*).

The relative levels of keratin expression were compared in the livers of the transgenic lines and normal nontransgenic FVB/N mice by examining the total keratin pool using high salt extraction (Fig. 1 *B*) and total liver homogenates (not shown). In TG2 mice, ~80% of the type I keratins (i.e., the total human ectopic and endogenous mouse K18) is human K18 whereas in the S52A mice ~70% of the total keratin is human K18. Both S52A lines express similar human K18 levels that in turn are slightly lower than those noted in TG2 mice. The endogenous levels of mouse K18 in TG2 and S52A mice, relative to wild-type mice, are decreased in proportion to the increased levels of ectopic human K18 such that the total type I keratins remains essentially constant (not shown). Overall and upon normalization of protein levels, type II keratin levels are also similar in TG2, S52A, and wild-type mice. Assignment of individual keratin bands was done by immunoblotting with anti-human and -mouse keratin-specific antibodies (e.g., Fig. 1 *B* and data not shown). The similarity of the keratin protein levels was also supported by the transgene copy number and by Northern blot analy-

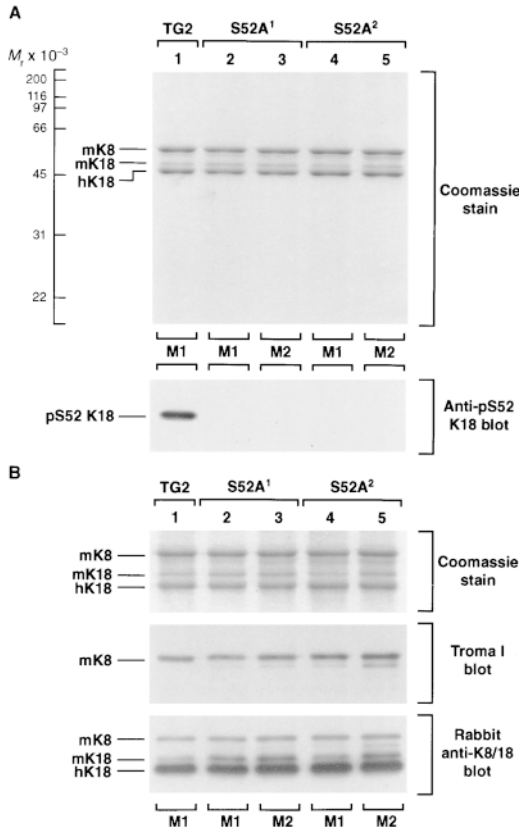

Figure 1. Characterization and expression of K18 S52A in transgenic mice. (*A*) Livers from transgenic mice that express WT K18 (TG2) or ser52→ala K18 (two independent transgenic lines $S52A^1$, $S52A^2$) were isolated followed by K8/18 immunoprecipitation using mAb L2A1 as described in Materials and Methods. M1 and M2 correspond to independent mice that were used from the indicated lines. Although mAb L2A1 recognizes human (*h*) but not mouse (*m*) K18, the mouse K8 and K18 copolymerize with hK18 in cells and therefore coprecipitate together. K8/18 precipitates were analyzed by SDS-PAGE followed by Coomassie staining, or were transferred to a PVDF membrane followed by immunoblotting with Ab 3055 that recognizes human phospho-ser52 of K18. Ab 3055 does not cross-react with the mouse equivalent of human phospho-ser52 K18 since the context of the sequence of the analogous phosphorylation site in mouse K18 is slightly different (35, 48). (*B*) Livers similar to those used in *A* were removed followed by high salt extraction of the keratin fraction as described in Materials and Methods. Keratin extracts, which include endogenous mouse and the transgene human K18 product, were analyzed by SDS-PAGE then Coomassie staining, and blotted with Troma I antibody (which recognizes mouse K8) or with rabbit anti–human K8/18 antibody that also recognizes mouse keratins.

sis to quantitate human K18 mRNA levels (not shown). The correlation between copy number, RNA and protein levels indicate that the S52A mutation does not have a significant effect on keratin protein turnover.

As part of the initial characterization of the phenotype of the S52A mice, we examined the histology and keratin immunofluorescence staining pattern of simple epithelial organs that express K8/18 including liver, kidney, pancreas, salivary gland and intestine. No histologic abnormality was noted in these organs and no differences were noted in animal weight or keratin staining pattern (not shown). In addition, hepatocyte viability after liver perfusion was >90% (n = 3 for each mouse line) for the TG2 and S52A lines, in contrast with the ~20% viability that is seen in transgenic mice that express K18 arg89→cys that results in disruption of the keratin filament network (25).

Basal and Post-Hepatectomy K18 Phosphorylation in TG2 and S52A Mice

We compared the overall basal K18 phosphorylation in TG2 mice (which express WT K18) and S52A mice (which express S52A→K18) using two-dimensional isoelectric focusing/SDS-PAGE analysis. Previous tryptic phosphopeptide mapping studies of K18 that was isolated from cultured human HT29 cells showed that the major radiolabeled K18 phosphopeptide corresponds to ser52 phosphorylation (e.g., Fig. 2 *A*; reference 28). This is also the major phosphopeptide in K18-transfected NIH-3T3 cells (Fig. 2 *C*) and in K18 that is purified from TG2 $^{32}PO_4$-labeled hepatocytes (Fig. 2 *B*). As shown in Fig. 3 *A*, WT K18 in TG2 mice (*a*) or in HT29 cells (*d*) has 3 major isoforms (isoforms no. 2 and no. 3 are not as well resolved in *d* as in *a*), whereas ser52→ala K18 in S52A mice (*b*) or in transfected NIH-3T3 cells (not shown) lack isoform no. 3. The assignment of the isoforms in Fig. 3 *A* (*a–d*) was confirmed by mixing a + b and d + e samples followed by two-dimensional gel analysis (not shown). This suggests that isoform no. 3 (in this basal phosphorylation state as compared with Figs. 5 and 6) corresponds to K18 that is primarily phosphorylated on ser52, and indicates that no significant compensatory phosphorylation has taken place in vivo in the transgenic mice. Isoform no. 3 also disappears upon treatment of K8/18 immunoprecipitates from HT29 cells (Fig. 3 *A*, *e*) or from TG2 livers (not shown) with alkaline phosphatase, and immune reactivity to two anti-phospho-K18 antibodies is almost completely abolished upon alkaline phosphatase treatment (Fig. 3 *B*). The precise nature of K18 isoform no. 2 is not known, but it is not routinely resolved from isoform no. 3 (e.g., Fig. 3 *A*, *c*) and therefore can be mistakenly considered as a phosphorylated isoform whereas it is more likely to represent a unique posttranslational modification. In support of this, isoform no. 2 does not label in vivo upon metabolic labeling with $^{32}PO_4$, is not affected by alkaline phosphatase, and is not recognized by two anti-phosphokeratin antibodies but is recognized by an anti-pan-K18 antibody (data not shown but summarized schematically in Fig. 3 *A*, *f*).

We used the post-hepatectomy liver regeneration mouse model to examine changes in K18 phosphorylation and organization during mitosis, and the effect of the ser52→ala mutation on liver regeneration. This is based on the mitosis-associated observed increase in K18 ser52 phosphorylation in cultured cells (37) and mice (27), and the apparent role in filament reorganization in cultured cells upon colcemid treatment of cells (23). As shown in Fig. 4 *A*, minimal K18 incorporation of $^{32}PO_4$ was observed in the S52A mice, as compared with TG2 mice pre- and post-hepatectomy, whereas changes in other phosphorylation sites such as K18 ser33 or K8 ser73 were not significantly affected. In addition, K8/18 phosphorylation in the S52A mice appeared appropriate after partial hepatectomy, in

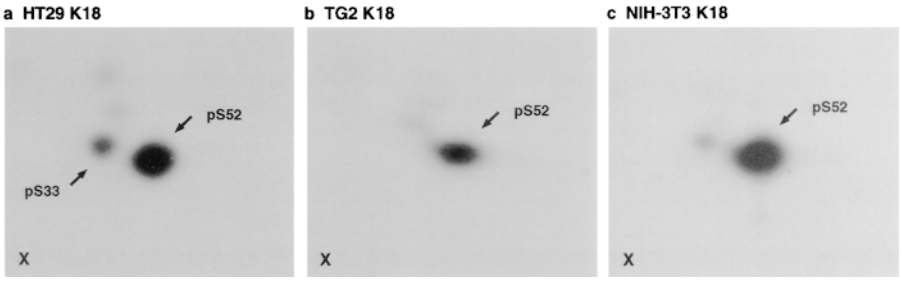

Figure 2. Peptide mapping of human K18 that is isolated from HT29 cells, TG2 mouse livers or from NIH-3T3 transfected cells. Hepatocytes were isolated from TG2 mice by liver perfusion for primary culture, and NIH-3T3 were cotransfected with WT K8/18. Hepatocytes, HT29 cells, or transfected NIH-3T3 cells were labeled with $^{32}PO_4$ followed by isolation of K8/18 immunoprecipitates then processing for K18 phosphopeptide mapping as described in Materials and Methods. Small x indicates location where sample was loaded. Arrows point to the ser52- or ser33-containing phosphopeptides. Assignment of the ser52-containing phosphopeptide was done by mixing samples a + b or a + c then peptide mapping (not shown). Assignment of pS33 was reported previously (30).

that an acidic shift in K8 and K18 isoforms was noted that is consistent with K8/18 hyperphosphorylation (Fig. 4 *C*). A similar shift was also noted in TG2 mouse K8/18 pre- and post-hepatectomy (27 and data not shown). There was no detectable difference in the ability of the S52A[1] and S52A[2] mouse lines to regenerate their livers as compared with TG2 mice (not shown), and a similar number of mitotic bodies were noted after partial hepatectomy (Fig. 4 *B*). Furthermore, no differences in keratin hepatocyte immunofluorescence staining were noted before or after partial hepatectomy (not shown). This indicates that the increase in K18 ser52 phosphorylation during mitosis does not appear to play an obvious significant role in the filament organization or progression through mitosis in intact animals.

Effect of K18 ser52 Phosphorylation in TG2 and S52A Mice on Susceptibility to Drug-induced Liver Injury

We tested the effect of two known hepatotoxins, griseofulvin (GF) and microcystin-LR (MLR), on TG2 and S52A transgenic mice. These drugs were chosen because of their dramatic toxic effect on the liver in association with K8/18 hyperphosphorylation (27, 52). TG2 and S52A mice were fed GF mixed with the normal mouse diet. After 17 d, the TG2 and S52A mice hyperphosphorylated their K18 similarly, as reflected by two-dimensional gel analysis (Fig. 5 *B*). As noted previously, K18 ser52 phosphorylation does not significantly change in TG2 mice after 17 d of GF feeding (27; Fig. 5 *A*, lanes *i–l*), but there is some ser52 dephosphorylation early on upon exposure of the TG2 mice to

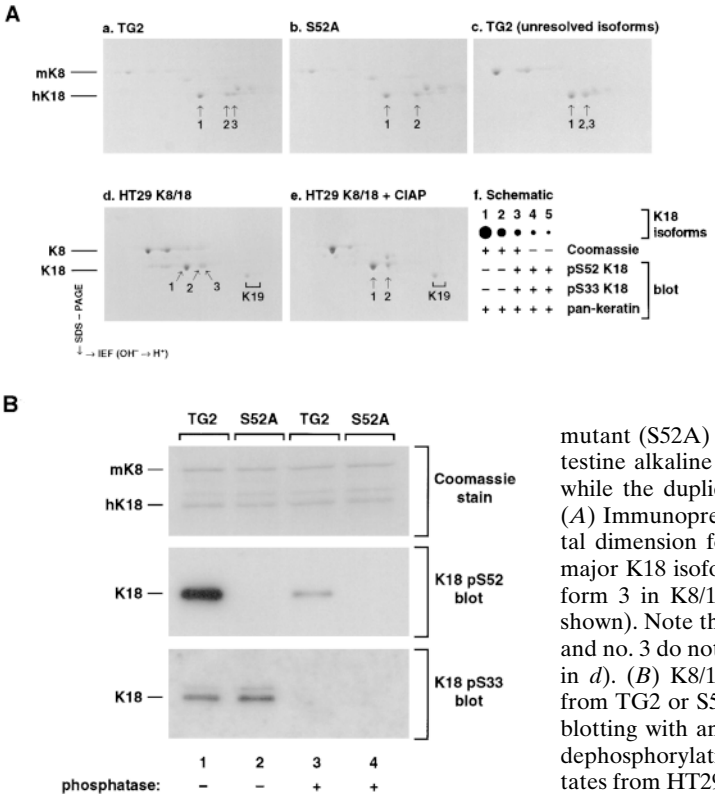

Figure 3. Dephosphorylation and two-dimensional gel analysis of WT and ser52→ala K18 that are isolated from HT29 cells and transgenic mice. K8/18 immunoprecipitates (in duplicate) were obtained from HT29 cells or from transgenic mice that overexpress WT or phosphorylation mutant (S52A) K18. One of the immunoprecipitates was treated with calf intestine alkaline phosphatase (CIAP) as described in Materials and Methods, while the duplicate was incubated with the dephosphorylation buffer alone. (*A*) Immunoprecipitates were analyzed by isoelectric focusing in the horizontal dimension followed by SDS-PAGE in the vertical dimension. The three major K18 isoforms are numbered 1, 2, and 3. CIAP treatment abolishes isoform 3 in K8/18 precipitates from HT29 cell (*e*) and from TG2 mice (not shown). Note that depending on the separation conditions, K18 isoforms no. 2 and no. 3 do not resolve (as shown in *c*) or resolve somewhat poorly (as shown in *d*). (*B*) K8/18 precipitates (±phosphatase treatment) that were obtained from TG2 or S52A mice were analyzed by SDS-PAGE followed by immunoblotting with anti-pS52 or anti pS33 K18 antibodies. Note the near complete dephosphorylation of pS33 and pS52 of K18. Blotting of similar K8/18 precipitates from HT29 cells gave similar results (not shown).

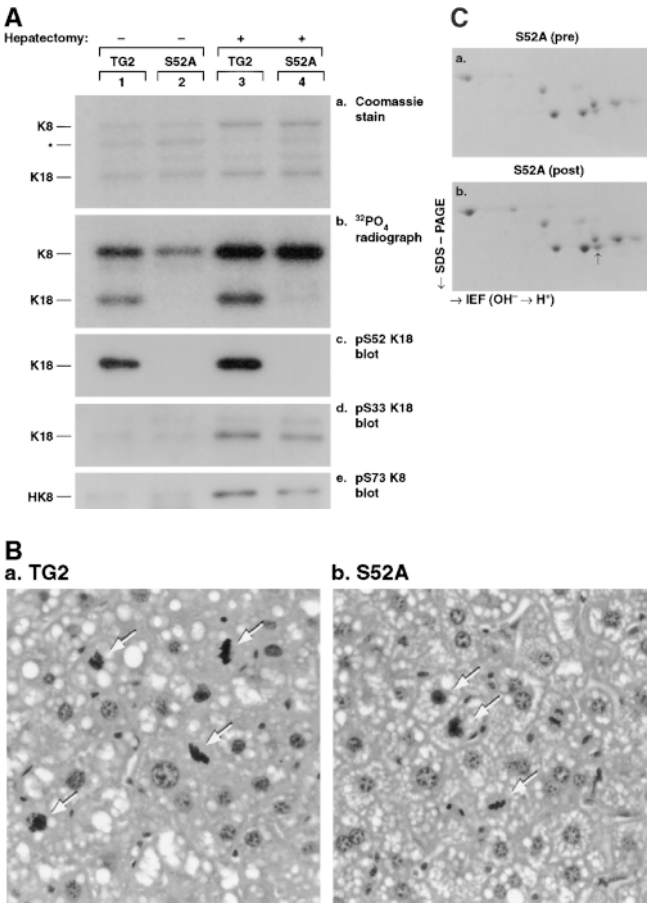

Figure 4. Analysis of keratin phosphorylation in vivo in transgenic mice that express WT or S52A K18, before and after hepatectomy. (*A*) TG2 and S52A mice were subjected to partial hepatectomy as described in Material and Methods. After 66 h, the regenerating livers were removed and a portion was fixed in 10% formalin for the hematoxylin and eosin staining shown in *B* and the remaining portion was used for metabolic labeling with $^{32}PO_4$. TG2 and S52A nonhepatectomized mouse livers were also similarly labeled (250 μCi/ml, 5 h) followed by solubilization with 1% Emp then immunoprecipitation of K8/18. Precipitates were analyzed by SDS-PAGE then Coomassie staining (*a*), autoradiography (*b*), or by immunoblotting with: Ab 3055 which recognizes K18 pS52 (*c*), Ab 8250 which recognizes K18 pS33 (*d*), or mAb LJ4 which recognizes K8 pS73 (*e*). K8 ser73 phosphorylation was shown previously to be a marker of mitotic cells in culture and in regenerating mouse liver (40). Asterisk in panel a corresponds to a degradation product of K8. (*B*) Livers from TG2 and S52A[1] mice that underwent hepatectomy in *A* were stained with hematoxylin and eosin. Arrows indicate mitotic bodies. Livers from S52A[2] mice had a similar number of mitotic bodies post-hepatectomy (not shown). (*C*) K8/18 immunoprecipitates were obtained from S52A[1] mice pre- and 72 h post-hepatectomy then examined by two-dimensional gel analysis. Of note, similar K8/18 precipitates that were obtained from S52A[2] and TG2 mice (before and after 72 h hepatectomy) showed a similar isoform pattern shift except for the absence of isoform no. 3 in K18 from S52A[2] mice (not shown). Arrow in panel b highlights the increased intensity of a K18 isoform, consistent with its increased phosphorylation.

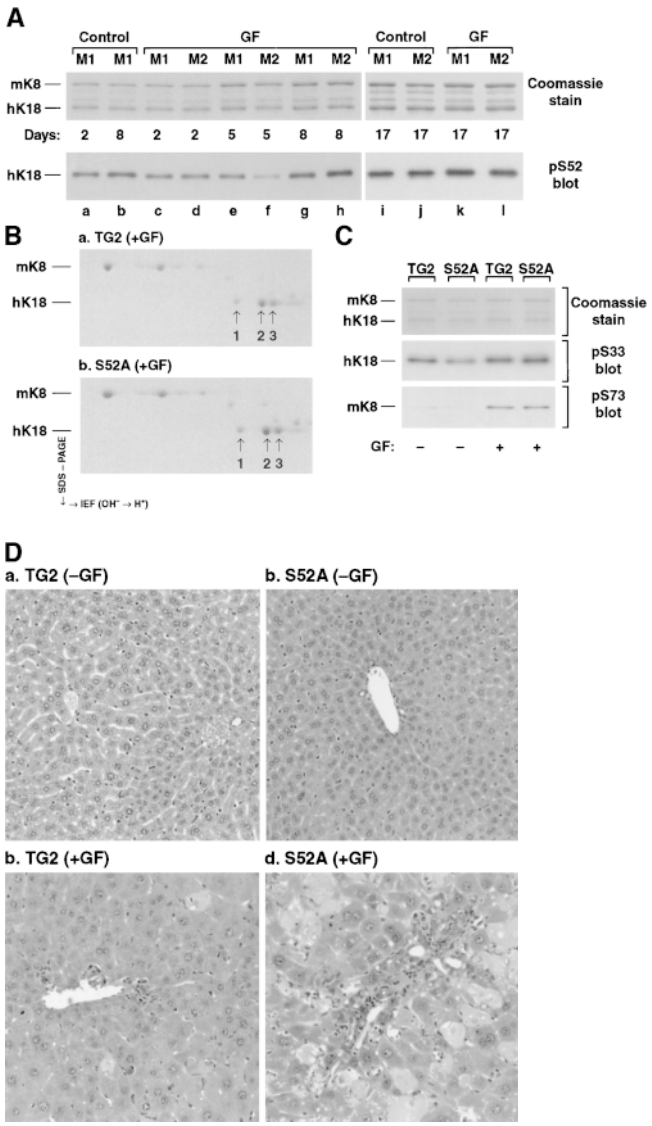

Figure 5. Effect of GF on liver histology and keratin phosphorylation in TG2 and S52A mice. (*A*) K8/18 precipitates were obtained from GF-fed TG2 mice after 2, 5, 8, or 17 d or from control diet-fed mice. M1 and M2 correspond to independent mice that were used from the indicated lines. The precipitates were separated by SDS-PAGE followed by Coomassie staining or were transferred to a PVDF membrane then blotted with anti-K18-pS52 Ab. *m* and *h* indicate mouse and human keratins, respectively. (*B*) K8/18 immunoprecipitates were obtained from 17-d GF-fed TG2 and S52A[1] mice, followed by two-dimensional gel analysis. Note the similar shift in isoforms in *a* and *b*, and the significant acidic shift for both relative to K8/18 that is isolated from the non-GF-fed control mice (shown in Fig. 3 *A*). (*C*) K8/18 immunoprecipitates were obtained from TG2 and S52A mouse livers (±GF) as in *A*. Precipitates were blotted with Ab 8250 and mAb LJ4 that recognize K18 pS33 and K8 pS73, respectively. (*D*) Formalin-fixed livers from TG2 and S52A mice fed control diet (−GF) or GF-containing diet (+GF) for 17 d were sectioned then stained with hematoxylin and eosin.

GF (Fig. 5 *A*, lanes *a–h*). However, maintaining a level of K18 ser52 phosphorylation does appear to be important in helping the hepatocyte cope with this drug-induced stress since S52A mice had more significant necrosis than TG2 mice (Fig. 5 *D* and Table I). The necrotic cells are easily discerned by their pale cytoplasmic color and virtual absence of nuclei. The mice had no GF-related mortality, and the dramatic increase in liver weight and liver-related

Table I. Comparison of Statistically Significant Differences in Phenotype Among GF- and MLR-treated TG2 and S52A Mice

	GF Diet	MLR Administration		
	Necrosis score	Vacuolization score	Hemorrhage score	Alkaline phosphatase
TG2 mice	10.3 ± 8.2	0.30 ± 0.48	0.60 ± 0.70	267 ± 23
S52A mice	23.7 ± 28.3	1.33 ± 0.50	1.60 ± 0.84	166 ± 17
p value	0.01	0.001	0.01	0.0001

The table shows only the parameters for which there was a statistically significant difference when comparing TG2 with S52A mice. No necrosis, vacuolization, or hemorrhage were noted in TG2 or S52A mice that were not given GF or MLR (not shown but see Fig. 5). For each treatment (i.e., control, GF or MLR), 10 mice were analyzed. Some of the standard deviations were high because of a few animals that had high parameters. Of note, alkaline phosphatase (U/L) was the only laboratory parameter that showed a significant difference among the serum tests that were examined (see Materials and Methods). The alkaline phosphatase values in control TG2 and S52A mice ($n = 8$ from each line) were similar (131 ± 6 and 123 ± 6, respectively).

serum enzymes were similar when comparing TG2 with S52A mice (not shown). Of note, $S52A^1$ and $S52A^2$ mice had a very similar liver histologic response to GF (not shown). No significant differences in K18 ser33 and K8 ser73 phosphorylation were noted between GF-fed TG2 and S52A mice (Fig. 5 *C*).

A comparison of the response of TG2 and S52A mice to the hepatotoxin MLR was also carried out. As shown in Fig. 6 *A*, MLR is associated with a dramatic increase (threefold) in TG2 K18 ser52 phosphorylation as determined by immunoblotting with the 3055 Ab. K18 undergoes significant hyperphosphorylation in TG2 and S52A mice in response to MLR, as noted upon two-dimensional gel analysis, although isoform no. 3 in S52A K18 is not as prominent as in TG2 K18 (Fig. 6 *C*). Isoform no. 3 of K18 S52A (Fig. 6 *C*, *b*) likely represents unique phosphorylation (i.e., non-ser52) as compared with isoform no. 3 of WT K18 (Fig. 6 *C*, *a*). In contrast to the GF model, S52A mice manifested a higher increase in K8 ser73 and a marginal difference in K18 ser33 phosphorylation after MLR exposure as compared with TG2 mice (Fig. 6 *B*). More importantly, MLR administration resulted in significantly more dramatic liver injury in the S52A mice as compared with TG2 mice (Fig. 6 *D* and Table I). The more dramatic liver injury noted in S52A mice involved all the MLR-associated histologic features, including vacuolization, necrosis, and hemorrhage (Table I) that have been well described in TG2, K18 arg89→cys, and K8-null mice (52). Necrotic pale-colored foci were primarily found near areas of hemorrhage (Fig. 6 *D*). The results of GF and MLR administration therefore indicate that blocking the phosphorylation of K18 ser52 in transgenic mice predisposes them to drug-induced liver injury.

Discussion

This study uses the overexpression of a keratin site-specific phosphorylation mutant in transgenic mice to demonstrate a physiologic role for keratin phosphorylation in protecting hepatocytes from drug-induced liver injury. Such a physiologic role is likely to apply to other IF proteins. To our knowledge, this is the first example of using transgenic mice to study the function of phosphorylation in a protein. This approach is likely to be informative for other proteins, particularly other IF proteins.

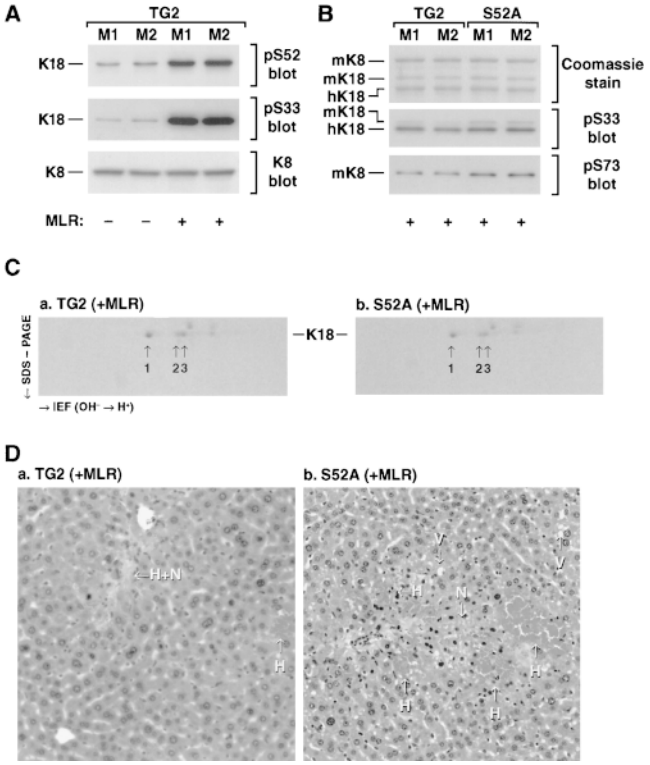

Figure 6. Effect of MLR on liver histology and keratin phosphorylation in TG2 and S52A mice. TG2 and S52A mice were given MLR in saline, or saline alone, by intraperitoneal injection followed by removal of the livers after 195 min as described in Materials and Methods. (*A*) Liver fragments were homogenized in Laemmli sample buffer or were solubilized in 1% Emp followed by immunoprecipitation. Equal amounts (10 μg) of total cell lysates from TG2 mice were separated by SDS-PAGE followed by blotting with anti-K18 pS52 or anti-pS33 Ab, or with anti-K8 antibody. A blot of nearly equal amounts of K8/18 precipitates (determined by Coomassie staining) gave a similar blotting pattern (not shown). M1 and M2 correspond to independent mice. (*B*) K8/18 immunoprecipitates were obtained from TG2 and S52A mouse livers, after MLR administration as in *A*. Precipitates were blotted with Ab 8250 and mAb LJ4 that recognize K18 pS33 and K8 pS73, respectively. (*C*) K8/18 immunoprecipitates were obtained from MLR-administered TG2 and S52A mice, followed by two-dimensional gel analysis. (*D*) Formalin-fixed livers from MLR-administered TG2 and S52A mice were sectioned then stained with hematoxylin and eosin.

General Properties of K18 Phosphorylation and Keratin Filaments in the K18 ser52→ala-expressing Transgenic Mice

As found in cultured cells, the K18 ser52-containing phosphopeptide is the major peptide that is labeled in transgenic mouse hepatocytes ex vivo (Fig. 2). Mutation of K18 ser52 followed by expression as a transgene product in mice resulted in the expected expression pattern (Fig. 1) without any evidence of compensatory phosphorylation of the endogenous mouse K18 (or K8) or compensatory phosphorylation of the human transgene K18 product at other sites (Figs. 3 and 4). No obvious effect on keratin filament assembly, or on desmoplakin or plectin distribution

was noted (not shown). We cannot exclude the possibility that altered phenotypes in keratin or other potential associated protein organization may have been obscured by the normal endogenous mouse K18. Addressing such a possibility may be feasible by breeding the S52A mice with the K18-null mice that have been reported by Magin et al. (42).

Analysis of the K18 isoforms by isoelectric focusing strongly suggests that K18 has an acidic modification, the nature of which remains to be defined. This modification results in the generation of isoform no. 2 (Fig. 3) that does not appear to be phosphorylated, based on resistance to dephosphorylation, lack of labeling by $^{32}PO_4$, and undetectable reactivity with two anti-phospho-K18 antibodies that recognize pS33 or pS52 (not shown). This isoform is physiologic in that it is seen in K18 that is expressed in mice and cultured human cells, is substoichiometric but easily detectable when isoelectric focusing separation conditions are favorable, and binds to a K18-specific antibody (not shown) thereby making it unlikely that it could correspond to another protein or to an alternate keratin or keratin degradation product.

Although changes in keratin phosphorylation in response to stress may appear at first glance to be global, several points deserve mention. First, the increase in keratin phosphorylation at multiple sites strongly suggests that this response is likely to act at several levels. For example, there appears to be distinct molecules of K18 that are phosphorylated at either ser52 or ser33 in mouse liver (30) thereby suggesting different functions. Indeed, one function for the K18 pS33 species is to bind 14-3-3 proteins and in doing so affect the subcellular partitioning and organization of keratin filaments (30, 36). Second, although changes in keratin phosphorylation occur at multiple sites and increase in the same site via a variety of modalities, some specificity and distinction is emerging. For example, apoptosis increases K8 and K18 phosphorylation at multiple sites (including K18 ser52) but does not affect K18 ser33 phosphorylation (28). In addition, studies in cultured HT29 cells showed that heat stress increases K18 phosphorylation primarily at non-ser52-containing sites, whereas phosphatase inhibitors increase K18 phosphorylation preferentially at ser52 (37).

Role of Keratin Phosphorylation in Providing Protection from Hepatotoxic Stress

The increase in K18 ser52 phosphorylation in response to the phosphatase inhibitors okadaic acid in cultured cells (37) and to MLR in TG2 mice (Fig. 6) raises at least four roles to consider for this hyperphosphorylation: (*a*) a bystander noncontributory role, (*b*) a toxicity protective role that in some ways may be considered similar to the induction of heat stress proteins, (*c*) a toxicity-promoting role, or (*d*) any sequential combination of *a–c*. The observed effect of increased susceptibility to liver injury in S52A as compared with TG2 mice, upon exposure to GF or MLR, provides in vivo evidence for the importance of K18 ser52 phosphorylation in modulating a protective role. The effect of the ser52 mutation is likely specific since other manipulations such as partial hepatectomy did not show a difference in liver regeneration between TG2 and S52A mice. We speculate that the mechanism of protection in the case of GF exposure is likely to be different than that in MLR exposure, since the latter is associated with a significant increase in K18 ser52 phosphorylation (Fig. 6). In contrast, GF exposure does not significantly affect ser52 phosphorylation when analyzed after 17 d, but decreases it slightly when analyzed after 5 d (Fig. 5). This suggests that the protective role of ser52 phosphorylation in the case of GF is likely to be indirect, as compared with MLR, and that steady state ser52 phosphorylation may play a role in initiating a cellular stress response in a fashion that could entail initial dephosphorylation depending on the stressful agent. Although the phenotype that we observe may simply be related to a structural defect that is caused by the mutation rather than a phosphorylation event per se, such a scenario is unlikely since the K18 ser52 mutant appears to assemble normally and can apparently reorganize in the context of mitosis without detectably affecting mitotic progression.

Previous clues to the importance of keratin and other IF protein phosphorylation in helping cells cope with stress are many, albeit correlative in nature. For example, in cultured cells, heat stress or rotavirus infection (37, 38), apoptosis (28), alcohol (21), or exposure to anti-microtubule agents (10) result in dramatic K8/18 hyperphosphorylation. Similarly, administration of GF to normal nontransgenic mice or transgenic normal mice that express WT K18 (i.e., the TG2 mouse line) results in significant K8/18 hyperphosphorylation (27). In contrast, transgenic mice that express a dominant negative K18 arg89→cys that results in keratin filament disruption are unable to hyperphosphorylate their keratins to the same extent as TG2 mice and are markedly more susceptible to GF-induced liver injury (25, 27). Association of increased neurofilament phosphorylation has also been correlated with stress in PC12 cells (16) and with aging in rats (17).

The mechanism by which K18 ser52 phosphorylation imparts protection from hepatotoxic stress now becomes an important question to address. Several hypotheses can be considered. For example, the K18 ser52 (and ser33)-phosphorylated species are preferentially found in the soluble and nonionic detergent extractable pool in cultured cells (26, 47), and under basal conditions ser52 phosphorylation is highly dynamic and is the predominant site that is labeled metabolically (Fig. 2). Therefore, the cellular location of ser52-phosphorylated K18 in these compartments may facilitate specific signaling events. Alternatively, keratin phosphorylation may act as a phosphate sink to protect cells from excess kinase activity (32), or may provide a phosphate reserve and help slow normal cellular processes until the stress subsides (26). The availability of the S52A transgenic mice should facilitate testing these hypotheses.

Potential Relevance of the GF and MLR Transgenic TG2 and S52A Mouse Models to Human Disease

The GF and MLR toxicity models tested herein have direct relevance to hepatotoxicity in humans, and highlight the potential for exploring K8/18 mutations in human idiopathic liver drug toxicity diseases. For example, a recently reported outbreak of liver failure and subsequent death in

nearly 50% of patients undergoing hemodialysis, at a facility in Brazil, resulted from inadvertent microcystin-contaminated water, with detectable levels of microcystin in serum and postmortem liver specimen (20). In addition, GF is a commonly used drug for treatment of patients with a variety of fungal infections (50). Despite the low GF toxicity level in humans versus animals, likely secondary to differences in the porphyrogenic effect between humans and mice (22), isolated cases of intrahepatic cholestasis after GF administration have been reported (9). The keratin mutation animal models that we have described to date, namely the K18 arg89→cys (25) and the K18 ser52→ala herein, both have increased susceptibility to drug-induced liver injury. Although to date only one cryptogenic liver disease patient with a K18 mutation that is associated with abnormal in vitro filament assembly has been described (29), the animal model data (27, 41, this study) do raise the possibility that K18 or K8 mutations may present clinically as a predisposition to hepatotoxicity upon specific environmental exposures. In this context, inability of keratins to undergo hyperphosphorylation, either directly (i.e., K18 ser52→ala mice) or indirectly (i.e., K18 arg89→cys mice), may provide one pathophysiologic explanation for this predisposition.

The observed statistically significant lack of an increase in serum alkaline phosphatase upon MLR exposure (Table I), but not upon GF exposure (not shown), was also seen in GF-fed mice that express K18 arg89→cys (~2,000 U/liter in GF-fed TG2 mice versus ~460 in K18 arg89→cys expressing mice; reference 27). In addition, K8-null mice also have lower levels of serum alkaline phosphatase as compared with control mice (4). The observed blunted alkaline phosphatase response in S52A as compared with TG2 mice suggests that keratin phosphorylation may play a role in this effect. However, it remains to be determined if this is a direct or indirect effect. To that end, changes in keratin phosphorylation could interfere with alkaline phosphatase secretion. Alternatively, the finding may simply reflect difference in necrosis such that situations of extensive necrosis (i.e., GF-fed K18 arg89→cys or MLR-administered S52A mice) result in limited spillage of the apically localized membrane associated enzyme, whereas situations of limited necrosis (i.e., GF-fed or MLR-administered TG2 mice) have the normal release of the enzyme. Differentiating between these and other possibilities should be feasible.

We are very grateful to Robert Oshima (The Burnham Institute, La Jolla, CA) for the use of the TG2 mice and for providing anti-mouse K18 antibodies, Harald Herrmann (German Cancer Research Center, Heidelberg, Germany) and Manijeh Pasdar (Universitsy of Alberta, Alberta, Canada) for their generous gifts of antibodies, Kris Morrow for preparing the figures, Marta Raygoza for animal breeding and care, Ron Van Groningen for serum testing, Romola Breckenridge for assisting with manuscript preparation, and Steve Avolicino (Histo-Tec Laboratory, Hayward, CA) for performing the histology staining.

This work was supported by Veterans Administration Merit and Career Development Awards (S.A. Michie and M.B Omary), National Institutes of Health grant DK-47918 (M.B. Omary), and Digestive Disease Center grant DK-38707.

Received for publication 21 August 1998 and in revised form 20 October 1998.

References

1. Abe, M., and R.G. Oshima. 1990. A single human keratin 18 gene is expressed in diverse epithelial cells of transgenic mice. *J. Cell Biol.* 111: 1197–1206.
2. Achtstaetter, T., M. Hatzfeld, R.A. Quinlan, D.C. Parmelee, and W.W. Franke. 1986. Separation of cytokeratin polypeptides by gel electrophoretic and chromatographic techniques and their identification by immunoblotting. *Methods Enzymol.* 134:355–371.
3. Albers, K.M., F.E. Davis, T.N. Perrone, E.Y. Lee, Y. Liu, and M. Vore. 1995. Expression of an epidermal keratin protein in liver of transgenic mice causes structural and functional abnormalities. *J. Cell Biol.* 128: 157–169.
4. Baribault, H., J. Penner, R.V. Iozzo, and M. Wilson-Heiner. 1994. Colorectal hyperplasia and inflammation in keratin 8-deficient FVB/N mice. *Genes Dev.* 8:2964–2973.
5. Baribault, H., J. Price, K. Miyai, and R.G. Oshima. 1993. Mid-gestational lethality in mice lacking keratin 8. *Genes Dev.* 7:1191–1202.
6. Bonifas, J.M., A.L. Rothman, and E.H. Epstein, Jr. 1991. Epidermolysis bullosa simplex: evidence in two familes for keratin gene abnormalities. *Science*. 254:1202–1205.
7. Boyle, W.J., P. Van Der Geer, and T. Hunter. 1991. Phosphopeptide mapping and phosphoamino acid analysis by two-dimensional separation on thin layer cellulose plates. *Methods Enzymol.* 201:110–149.
8. Caulin, C., G.S. Salvesen, and R.G. Oshima. 1997. Caspase cleavage of keratin 18 and reorganization of intermediate filaments during epithelial cell apoptosis. *J. Cell Biol.* 138:1379–1394.
9. Chiprut, R.O., A. Viteri, C. Jamroz, and W.P. Dyck. 1976. Intrahepatic cholestasis after griseofulvin administration. *Gastroenterology.* 70:1141–1143.
10. Chou, C.-F., and M.B. Omary. 1993. Mitotic-arrest associated enhancement of O-linked glycosylation and phosphorylation of human keratins 8 and 18. *J. Biol. Chem.* 268:4465–4472.
11. Chou, C.-F., A.J. Smith, and M.B. Omary. 1992. Characterization and dynamics of O-linked glycosylation of human cytokeratin 8 and 18. *J. Biol. Chem.* 267:3901–3906.
12. Clayton, D.F., and J.E. Darnell, Jr. 1983. Changes in liver-specific compared to common gene transcription during primary culture of mouse hepatocytes. *Mol. Cell. Biol.* 3:1552–1561.
13. Coulombe, P.A., M.E. Hutton, A. Letai, A. Hebert, A.S. Paller, and E. Fuchs. 1991. Point mutations in human keratin 14 genes of epidermolysis bullosa simplex patients: genetic and functional analysis. *Cell*. 66:1301–1311.
14. Fuchs, E., and K. Weber. 1994. Intermediate filaments: structure, dynamics, function and disease. *Annu. Rev. Biochem.* 63:345–382.
15. Fuchs, E., and D.W. Cleveland. 1998. A structural scaffolding of intermediate filaments in health and disease. *Science.* 279:514–519.
16. Glasson, B.I., and W.E. Mushynski. 1996. Aberrant stress-induced phosphorylation of perikaryal neurofilaments. *J. Biol. Chem.* 271:30404–30409.
17. Gou, J.-P., J. Eyer, and J.-F. Leterrier. 1995. Progressive hyperphosphorylation of neurofilament heavy subunits with aging: Possible involvement in the mechanism of neurofilament accumulation. *Biochem. Biophys. Res. Commun.* 215:368–376.
18. Inagaki, M., N. Inagaki, T. Takahashi, and Y. Takai. 1997. Phosphorylation-dependent control of structures of intermediate filaments: a novel approach using site-and phosphorylation state-specific antibodies. *J. Biochem.* 121:407–414.
19. Irvine, A.D., L.D. Corden, O. Swensson, B. Swensson, J.E. Moore, D.G. Frazer, F.J.D. Smith, R.G. Knowlton, E. Christophers, R. Rochels, et al. 1997. Mutations in cornea-specific keratin K3 or K12 genes cause Meesmann's corneal dystrophy. *Nat. Genet.* 16:184–187.
20. Jochimsen, E.M., W.W. Carmichael, J.-S. An, D.M. Cardo, S.T. Cookson, C.E.M. Holmes, M.B.C. Antunes, D.A.M. Filho, T.M. Lyra, V.S.T. Barreto, et al. 1998. Liver failure and death after exposure to microcystins at a hemodialysis center in Brazil. *N. Engl. J. Med.* 338:873–878.
21. Kawahara, H., M. Cadrin, and S.W. French. 1990. Ethanol-induced phosphorylation of cytokeratin in cultured hepatocytes. *Life Sci.* 47:859–863.
22. Knasmuller, S., W. Parzefall, C. Helma, F. Kassle, S. Ecker, and R. Schulte-Herrmann. 1997. Toxic effects of griseofulvin: disease models, mechanisms, and risk assessment. *Crit. Rev. Toxicol.* 27:495–537.
23. Ku, N.-O., and M.B. Omary. 1994. Identification of the major physiologic phosphorylation site of human keratin 18: potential kinases and a role in filament reorganization. *J. Cell Biol.* 127:161–171.
24. Ku, N.-O., and M.B. Omary. 1997. Phosphorylation of human keratin 8 *in vivo* at conserved head domain serine 23 and at epidermal growth factor-stimulated tail domain serine 431. *J. Biol. Chem.* 272:7556–7564.
25. Ku, N.-O., S. Michie, R.G. Oshima, and M.B. Omary. 1995. Chronic hepatitis, hepatocyte fragility, and increased soluble phosphoglycokeratins in transgenic mice expressing a keratin 18 conserved arginine mutant. *J. Cell Biol.* 131:1303–1314.
26. Ku, N.-O., J. Liao, C.-F. Chou, and M.B. Omary. 1996. Implications of intermediate filament protein phosphorylation. *Cancer Metast. Rev.* 15:429–444.
27. Ku, N.-O., S.A. Michie, R.M. Soetikno, E.Z. Resurreccion, R.L. Broome,

R.G. Oshima, and M.B. Omary. 1996. Susceptibility to hepatotoxicity in transgenic mice that express a dominant-negative human keratin 18 mutant. *J. Clin. Invest.* 98:1034–1046.
28. Ku, N.-O., J. Liao, and M.B. Omary. 1997. Apoptosis generates stable fragments of type I keratins. *J. Biol. Chem.* 273:33197–33203.
29. Ku, N.-O., T.L. Wright, N.A. Terrault, R. Gish, and M.B. Omary. 1997. Mutation of human keratin 18 in association with cryptogenic cirrhosis. *J. Clin. Invest.* 99:19–23.
30. Ku, N.-O., J. Liao, and M.B. Omary. 1998. Phosphorylation of human keratin 18 serine -33 regulates binding to 14-3-3-proteins. *EMBO (Eur. Mol. Biol. Organ.) J.* 17:1892–1906.
31. Laemmli, U.K. 1970. Cleavage of structural proteins during the assembly of the head of bacteriophage T4. *Nature*. 227:680–685.
32. Lai, Y.-K., W.-C. Lee, and K.-D. Chen. 1993. Vimentin serves as a phosphate sink during the apparent activation of protein kinases by okadaic acid in mammalian cells. *J. Cell. Biochem.* 53:161–168.
33. Lane, E.B., E.L. Rugg, H. Navsaria, I.M. Leigh, A.H.M Heagerty, A. Ishida-Yamamoto, and R.A.J. Eady. 1992. A mutation in the conserved helix termination peptide of keratin 5 in hereditary skin blistering. *Nature.* 356:244–246.
34. Lazarides, E. 1980. Intermediate filaments as mechanical integrators of cellular space. *Nature.* 283:249–256.
35. Leube, R.E., F.X. Bosch, V. Romano, R. Zimbelmann, H. Hofler, and W.W. Franke. 1986. Cytokeratin expression in simple epithelia III: detection of mRNAs encoding human cytokeratins nos. 8 and 18 in normal and tumor cells by hybridization with cDNA sequences in vitro and in situ. *Differentiation.* 33:69–85.
36. Liao, J., and M.B. Omary. 1996. 14-3-3 proteins associate with phosphorylated simple epithelial keratins during cell cycle progression and act as a solubility cofactor. *J. Cell Biol.* 133:345–358.
37. Liao, J., L.A. Lowthert, N.-O. Ku, R. Fernandez, and M.B. Omary. 1995. Dynamics of human keratin 18 phosphorylation: polarized distribution of phosphorylated keratins in simple epithelial tissues. *J. Cell Biol.* 131: 1291–1301.
38. Liao, J., L.A. Lowthert, and M.B. Omary. 1995. Heat stress or rotavirus infection of human epithelial cells generates a distinct hyperphosphorylated forms of keratin 8. *Exp. Cell Res.* 219:348–357.
39. Liao, J., N.-O. Ku, and M.B. Omary. 1996. Two-dimensional gel analysis of glandular keratin intermediate filament phosphorylation. *Electrophoresis.* 17:1671–1676.
40. Liao, J., N.-O. Ku, and M.B. Omary. 1997. Stress, apoptosis, and mitosis induce phosphorylation of human keratin 8 at ser73 in tissues and cultured cells. *J. Biol. Chem.* 272:17565–17573.
41. Loranger, A., S. Duclos, A. Grenier, J. Price, M. Wilson-Heiner, H. Baribault, and N. Marceau. 1997. Simple epithelium keratins are required for maintenance of hepatocyte integrity. *Am. J. Pathol.* 151:1673–1683.
42. Magin, T.M., R. Schroder, S. Leitgeb, F. Wanninger, K. Zatloukal, C. Grund, and D.W. Melton. 1998. Lessons from keratin 18 knockout mice: formation of novel keratin filaments, secondary loss of keratin 7 and accumulation of liver-specific keratin 8-positive aggregates. *J. Cell Biol.* 140:1441–1451.
43. McLean, W.H.I., and E.B. Lane. 1995. Intermediate filaments in disease. *Curr. Opin. Cell Biol.* 7:118–125.
44. Moll, R., W.W. Franke, D.L. Schiller, B. Geiger, and R. Krepler. 1982. The catalog of human cytokeratins: patterns of expression in normal epithelia, tumors and cultured cells. *Cell.* 31:11–24.
45. Ohta, T., R. Nishiwaki, J. Yatsunami, A. Komori, M. Suganuma, and M. Fujiki. 1992. Hyperphosphorylation of cytokeratins 8 and 18 by microcystin-LR, a new liver rumor promoter, in primary cultured rat hepatocytes. *Carcinogenesis.* 13:2443–2447.
46. Omary, M.B., and N.-O. Ku. 1997. Intermediate filament proteins of the liver: emerging disease association and functions. *Hepatology.* 25:1043–1048.
47. Omary, M.B., N.-O. Ku, J. Liao, and D. Price. 1998. Keratin modifications and solubility properties in epithelial cells and in vitro. *In* Subcellular Biochemistry. Vol. 31: Intermediate Filaments. H. Herrmann, and I. Harris, editors. Plenum Press, New York. 105–139.
48. Oshima, R.G., J.L. Milan, and G. Cecena. 1986. Comparison of mouse and human keratin 18: a component of intermediate filaments expressed prior to implantation. *Differentiation.* 33:61–68.
49. Steinert, P.M., and D.R. Roop. 1988. Molecular and cellular biology of intermediate filnments. *Annu. Rev. Biochem.* 57:593–625.
50. Tanz, R.R., A.A. Hebert, and N.B. Esterly. 1988. Treating tinea capitis: should ketoconazole replace griseofulvin. *J. Pediatr.* 112:987–991.
51. Toivola, D.M., R.D. Goldman, D.R. Garrod, and J.E. Eriksson. 1997. Protein phosphatases maintain the organization and structural interactions of hepatic keratin intermediate filaments. *J. Cell Sci.* 110:23–33.
52. Toivola, D.M., M.B. Omary, N.-O. Ku, O. Peltola, H. Baribault, and J.E. Eriksson. 1998. Protein phosphatase inhibition in normal and keratin 8/18 assembly-incompetent mouse strains supports a functional role of keratin intermediate filaments in preserving hepatocyte integrity. *Hepatology*. 28:116–128.
53. Towbin, H., T. Staehelin, and J. Gordon. 1979. Electrophoretic transfer of proteins from polyacrylamide gels to nitrocellulose sheets: procedures and some applications. *Proc. Natl. Acad. Sci. USA.* 76:4350–4354.
54. Vassar, R., P.A. Coulombe, L. Degenstein, K. Albers, and E. Fuchs. 1991. Mutant keratin expression in transgenic mice causes marked abnormalities resembling a human genetic skin disease. *Cell.* 64:365–380.
55. Wilson, M.E., R.E. Stowell, H.O. Yokoyama, and K.K. Tsuboi. 1953. Cytological changes in regenerating mouse liver. *Cancer Res.* 13:86–92.
56. Yokoyama, H.O., M.E. Wilson, K.K. Tsuboi, and R.E. Stowell. 1953. Regeneration of mouse liver after partial hepatectomy. *Cancer Res.* 13:80–85.